Comultiplication in link Floer homology
and transversely nonsimple links

JOHN A BALDWIN

For a word w in the braid group B_n, we denote by T_w the corresponding transverse braid in $(\mathbb{R}^3, \xi_{\mathrm{rot}})$. We exhibit, for any two $g, h \in B_n$, a "comultiplication" map on link Floer homology $\widetilde{\Phi}\colon \widetilde{HFL}(m(T_{hg})) \to \widetilde{HFL}(m(T_g \# T_h))$ which sends $\widetilde{\theta}(T_{hg})$ to $\widetilde{\theta}(T_g \# T_h)$. We use this comultiplication map to generate infinitely many new examples of prime topological link types which are not transversely simple.

1 Introduction

Transverse links feature prominently in the study of contact 3–manifolds. They arise very naturally – for instance, as binding components of open book decompositions – and can be used to discern important properties of the contact structures in which they sit (see Baker, Etnyre and Van Horn-Morris [1, Theorem 1.15] for a recent example). Yet, transverse links, even in the standard tight contact structure ξ_{std} on $\mathbb{R}^3$, are notoriously difficult to classify up to transverse isotopy.

A transverse link T comes equipped with two "classical" invariants which are preserved under transverse isotopy: its topological link type and its self-linking number $\mathrm{sl}(T)$. For transverse links with more than one component, it makes sense to refine the notion of self-linking number as follows. Let T and T' be two transverse representatives of some l–component topological link type, and suppose there are labelings $T = T_1 \cup \cdots \cup T_l$ and $T' = T'_1 \cup \cdots \cup T'_l$ of the components of T and T' such that

(1) there is a topological isotopy sending T to T' which sends T_i to T'_i for each i,

(2) $\mathrm{sl}(S) = \mathrm{sl}(S')$ for any sublinks $S = T_{n_1} \cup \cdots \cup T_{n_j}$ and $S' = T'_{n_1} \cup \cdots \cup T'_{n_j}$.

Then we say that T and T' have the same *self-linking data*, and we write $\mathcal{SL}(T) = \mathcal{SL}(T')$. A basic question in contact geometry is how to tell, given two transverse representatives T and T' of some topological link with the same self-linking data, whether T and T' are transversely isotopic; that is, whether the classical data completely determines the *transverse* link type. We say that a topological link type is *transversely simple* if any two transverse representatives T and T' which satisfy $\mathcal{SL}(T) = \mathcal{SL}(T')$ are transversely isotopic. Otherwise, the link type is said to be *transversely nonsimple*.

From this point on, we shall restrict our attention to transverse links in the tight rotationally symmetric contact structure ξ_{rot} on $\mathbb{R}^3$, which is contactomorphic to ξ_{std}. There are several well-known examples of knot types which are transversely simple. Among these are the unknot by Eliashberg [7], torus knots by Etnyre [9] and the figure eight by Etnyre and Honda [10].

Only recently, however, have knot types been discovered which are not transversely simple. These include a family of 3–braids found by Birman and Menasco [5] using the theory of braid foliations and the $(2,3)$ cable of the $(2,3)$ torus knot, which was shown to be transversely nonsimple by Etnyre and Honda using contact-geometric techniques [12]. Matsuda and Menasco have since identified two explicit transverse representatives of this cabled torus knot which have identical self-linking numbers, but which are not transversely isotopic [18]. Their examples take center stage in Section 5 of this paper.

There has been a flurry of progress in finding transversely nonsimple link types in the last couple years, spurred by the discovery of a transverse invariant θ in link Floer homology by Ozsváth, Szabó and Thurston [25]; this discovery, in turn, was made possible by the combinatorial description of HFL^- found by Manolescu, Ozsváth and Sarkar in [16] (see also Manolescu, Ozsváth, Szabó and Thurston [17]).[1] This θ invariant is applied by Ng, Ozsváth and Thurston in [20] to identify several examples of transversely nonsimple links, including the knot 10_{132}. In [28], Vértesi proves a connected sum formula for θ, which she wields to find infinitely many examples of nonprime knots which are transversely nonsimple (Kawamura has since proven a similar result without using Floer homology [13]; both hers and Vértesi's results follow from Etnyre and Honda's work on Legendrian connected sums [11]).

Finding infinite families of transversely nonsimple *prime* knots is generally more difficult. Using a slightly different invariant, which we shall denote by $\underline{\theta}$, derived from knot Floer homology and discovered by Lisca, Ozsváth, Szabó and Stipsicz in [15], Ozsváth and Stipsicz identify such an infinite family among two-bridge knots [23]. And, most recently, Khandhawit and Ng use the invariant θ to construct a 2–parameter infinite family of prime transversely nonsimple knots, which generalizes the example of 10_{132} [14].

In this paper, we formulate and apply a strategy for generating a slew of new infinite families of transversely nonsimple prime links. This strategy hinges on the "naturality" results below. For a word w in the braid group B_n, we denote by T_w the corresponding transverse braid in $(\mathbb{R}^3, \xi_{rot})$.

---

[1]There are several versions of this θ invariant, denoted by θ^-, $\widehat{\theta}$ and $\widetilde{\theta}$.

Theorem 1.1 *There exists a map on link Floer homology*

$$\widetilde{\Phi}\colon \widetilde{HFL}(m(T_{w\sigma_i})) \to \widetilde{HFL}(m(T_w))$$

which sends $\widetilde{\theta}(T_{w\sigma_i})$ *to* $\widetilde{\theta}(T_w)$, *where* σ_i *is one of the standard generators of* B_n.

This theorem implies the existence of a "comultiplication" map on link Floer homology, similar in spirit to the map which we discovered in [2]:

Theorem 1.2 *For any two braid words* h *and* g *in* B_n, *there exists a map*

$$\widetilde{\mu}\colon \widetilde{HFL}(m(T_{hg})) \to \widetilde{HFL}(m(T_g \# T_h))$$

which sends $\widetilde{\theta}(T_{hg})$ *to* $\widetilde{\theta}(T_g \# T_h)$.

One may combine Theorem 1.2 with Vértesi's result governing the behavior of θ under connected sums to conclude the following.

Theorem 1.3 *If* $\widehat{\theta}(T_g)$ *and* $\widehat{\theta}(T_h)$ *are both nonzero, then so is* $\widehat{\theta}(T_{hg})$.

Here, we sketch one potential way to use these results to find transversely nonsimple links. Start with some w_1, $w_2 \in B_n$ for which T_{w_1} and T_{w_2} are topologically isotopic and have the same self-linking data, but for which $\widehat{\theta}(T_{w_1}) = 0$ while $\widehat{\theta}(T_{w_2}) \neq 0$, so that T_{w_1} and T_{w_2} are not transversely isotopic. Now, choose an $h \in B_n$ for which $\widehat{\theta}(T_h) \neq 0$. Theorem 1.3 then implies that $\widehat{\theta}(T_{hw_2}) \neq 0$ as well. If one can show that $\widehat{\theta}(T_{hw_1}) = 0$, that T_{hw_1} and T_{hw_2} still represent the same topological link type, and that $\mathcal{SL}(T_{hw_1}) = \mathcal{SL}(T_{hw_2})$ (this is automatic if T_{hw_1} and T_{hw_2} are knots), then one may conclude that T_{hw_1} represents a transversely nonsimple link type.

An advantage of this approach for generating new transversely nonsimple link types from old over, say, that of Vértesi [28] and Kawamuro [13], is that there is no *a priori* reason to expect that the links so formed are composite. We demonstrate the effectiveness of this approach in Section 5 of this paper. In doing so, we describe an infinite family of prime transversely nonsimple link types (half are knots; the other half are 3–component links) which generalizes the $(2, 3)$ cable of the $(2, 3)$ torus knot. Moreover, it is clear that this example only scratches the surface of the potential of our more general technique.

Lastly, it is tempting to conjecture that the two invariants θ and $\underline{\theta}$ agree for transverse links in $(\mathbb{R}^3, \xi_{\text{rot}})$, as they share many formal properties. We prove a partial result in this direction, which follows from Theorem 1.1 together with work of Vela-Vick on the $\underline{\theta}$ invariant [27].

Theorem 1.4 $\widehat{\theta}(T)$ *and* $\underline{\widehat{\theta}}(T)$ *agree for positive, transverse, connected braids* T *in* $(\mathbb{R}^3, \xi_{\text{rot}})$.

Organization

In the next section, we outline the relationship between grid diagrams, Legendrian links and their transverse pushoffs. In Section 3, we review the grid diagram construction of link Floer homology and describe some important properties of the transverse invariant θ. In Section 4, we prove Theorems 1.1, 1.2, 1.3 and 1.4. And, in Section 5, we outline a general strategy for using our comultiplication result to produce new examples of transversely nonsimple link types, and we give an infinite family of such examples which are prime.

2   Grid diagrams, Legendrian and transverse links

In this section, we provide a brief review of the relationship between Legendrian links in $(\mathbb{R}^3, \xi_{\mathrm{std}})$, transverse braids in $(\mathbb{R}^3, \xi_{\mathrm{rot}})$ and grid diagrams, largely following the discussion in [14]. For a more detailed account, see Khandhawit and Ng [14] and Ng and Thurston [21]. The standard tight contact structure ξ_{std} on $\mathbb{R}^3$ is given as

$$\xi_{\mathrm{std}} = \ker(dz - y\,dx).$$

An oriented link $L \subset (\mathbb{R}^3, \xi_{\mathrm{std}})$ is called *Legendrian* if it is everywhere tangent to ξ_{std}, and *transverse* if it is everywhere transverse to ξ_{std} such that $dz - y\,dx > 0$ along the orientation of L. Any smooth link can be perturbed by a C^0 isotopy to be Legendrian or transverse. We say that two Legendrian (resp. transverse) links are *Legendrian* (resp. *transversely*) isotopic if they are isotopic through Legendrian (resp. transverse) links.

A Legendrian link L can be perturbed to a transverse link (which is arbitrarily close to L in the C^∞ topology) by pushing L along its length in a generic direction transverse to the contact planes in such a way that the orientation of the pushoff agrees with that of L. The resulting link L^+ is called a *positive transverse pushoff* of L. Legendrian isotopic links give rise to transversely isotopic pushoffs. Conversely, every transverse link is the positive transverse pushoff of some Legendrian link; however, two such Legendrian links need not be Legendrian isotopic. The precise relationship between Legendrian and transverse links is best explained via *front projections*.

The front projection of a Legendrian link is its projection onto the xz plane. The front projection of a generic Legendrian link has no vertical tangencies and has only

semicubical cusps and transverse double points as singularities. Moreover, at each double point, the slope of the overcrossing is more negative than the slope of the undercrossing. See Figure 2 (c) for the front projection of a right-handed Legendrian trefoil.

The *positive* (resp. *negative*) *stabilization* of a Legendrian link L along some component C of L is the Legendrian link whose front projection is obtained from that of L by adding a zigzag along C with downward (resp. upward) pointing cusps. See Figure 1. Two Legendrian links are said to be *negatively stably isotopic* if they are Legendrian isotopic after each has been negatively stabilized some number of times along some of its components. The following theorem implies that the classification of transverse links up to transverse isotopy is equivalent to the classification of Legendrian links up to Legendrian isotopy and negative stabilization.

Figure 1: (a) and (b) are local pictures of the positive and negative stabilizations, respectively, of a Legendrian link along one of its components C.

Theorem 2.1 [8; 22] *Two Legendrian links are negatively stably isotopic if and only if their positive transverse pushoffs are transversely isotopic.*

Consider the rotationally symmetric tight contact structure on $\mathbb{R}^3$ defined by

$$\xi_{\mathrm{rot}} = \ker(dz - y\,dx + x\,dy).$$

The diffeomorphism of $\mathbb{R}^3$ given by

$$(1) \qquad\qquad \phi(x, y, z) = (x, 2y, xy + z)$$

sends ξ_{rot} to ξ_{std}. One can define transverse links for ξ_{rot} in the same way that one does for ξ_{std}. Since ϕ sends a transverse link in $(\mathbb{R}^3, \xi_{\mathrm{rot}})$ to a transverse link in $(\mathbb{R}^3, \xi_{\mathrm{std}})$, the study of transverse links in $(\mathbb{R}^3, \xi_{\mathrm{std}})$ is equivalent to that in $(\mathbb{R}^3, \xi_{\mathrm{rot}})$; however, the latter is often more convenient, per the following theorem of Bennequin.

Theorem 2.2 [3] *Any transverse link in $(\mathbb{R}^3, \xi_{\mathrm{rot}})$ is transversely isotopic to a closed braid around the z–axis.*

Theorem 2.2 allows us to use braid-theoretic techniques to study transverse links. For a braid word $w \in B_n$, we let T_w denote the corresponding transverse braid around

the z–axis. Braid words which are conjugate in B_n clearly correspond to transversely isotopic links. Recall that, for $w \in B_n$, a *positive* (resp. *negative*) *braid stabilization* of w is the operation which replaces w by the word $w\sigma_n$ (resp. $w\sigma_n^{-1}$) in B_{n+1}. We will also refer to $T_{w\sigma_n}$ (resp. $T_{w\sigma_n^{-1}}$) as the *positive* (resp. *negative*) *braid stabilization* of the transverse link T_w. The following theorem makes precise the relationship between braids and transverse links in $(\mathbb{R}^3, \xi_{\mathrm{rot}})$.

Theorem 2.3 [22; 30] *For $w \in B_n$ and $w' \in B_m$, the transverse links T_w and $T_{w'}$ are transversely isotopic in $(\mathbb{R}^3, \xi_{\mathrm{rot}})$ if and only if w and w' are related by a sequence of conjugations and positive braid stabilizations and destabilizations.*

In Section 5, we use a braid operation called an *exchange move*. If a, b and c in B_n are words in the generators $\sigma_2, \dots, \sigma_{n-1}$, then an exchange move is the operation which replaces the word $w_1 = a\sigma_1 b\sigma_1^{-1} c$ with the word $w_2 = a\sigma_1^{-1} b\sigma_1 c$. An exchange move is actually just a composition of conjugations, one positive braid stabilization and one positive destabilization, and so the link T_{w_1} is transversely isotopic to T_{w_2} (see, for example, Ng and Thurston [21]).

It bears mentioning that the self-linking number of a transverse link admits a nice formulation in the language of braids. If Σ is a Seifert surface for a transverse link T, then the vector bundle $\xi_{\mathrm{rot}}|_\Sigma$ is trivial and, therefore, has a nonzero section v. Recall that the *self-linking number* of T is defined by

$$\mathrm{sl}(T) = \mathrm{lk}(T, T'),$$

where T' is a pushoff of T in the direction of v. Any two links which are transversely isotopic have identical self-linking numbers. For a word $w \in B_n$, the self-linking number of T_w is given simply by $a(w) - n$, where $a(w)$ is the algebraic length of w.

In what remains of this section, we describe a relationship between the front diagram of a Legendrian link in $(\mathbb{R}^3, \xi_{\mathrm{std}})$ and a braid representation of its positive transverse pushoff, thought of as a transverse link in $(\mathbb{R}^3, \xi_{\mathrm{rot}})$. Grid diagrams provide the necessary connection.

A *grid diagram* G is an $k \times k$ square grid along with a collection of k X's and k O's contained in these squares such that every row and column contains exactly one O and one X and no square contains both an O and an X. See Figure 2 (a). We call k the *grid number* of G. One can produce an oriented link diagram L from G by drawing a horizontal segment from the O's to the X's in each row and a vertical segment from the X's to the O's in each column so that the horizontal segments pass over the vertical segments (this is the convention used by Khandhawit and Ng [14], and the opposite of the convention in Manolescu, Ozsváth and Sarkar [16]; see Ng and

Thurston [21] for a discussion on the relationship between the two conventions), as in Figure 2 (b). By rotating L 45° clockwise, and then smoothing the upward and downward pointing corners and turning the leftward and rightward pointing corners into cusps, one obtains the front projection of a Legendrian link, as in Figure 2 (c). Let us denote this Legendrian link by $L(G)$.
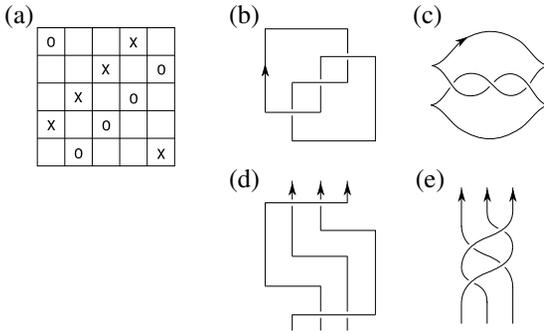

Figure 2: In (a), a grid diagram G. In (b), the oriented link corresponding to G. In (c), a front projection for the Legendrian link $L(G)$. In (d) and (e), the braid corresponding to G. Here, $w(G) = \sigma_1\sigma_2\sigma_1\sigma_2$.

Alternatively, one can construct a braid diagram from G by drawing a horizontal segment from the O's to the X's in each row, as before, and drawing a vertical segment from the X's to the O's for each column in which the marking X lies under the marking O. For those columns in which the X is above the O, we draw two vertical segments: one from the X up to the top of the grid diagram, and the other from the bottom of the grid diagram up to the O. As before, we require that the horizontal segments pass over the vertical segments. Note that all vertical segments are oriented upwards and that the closure of the diagram we have constructed is a braid. See Figures 2 (d) and 2 (e) for an example of this procedure. Let us denote the corresponding braid word by $w(G)$, read from the bottom up. The relationship between $T_{w(G)}$ and $(L(G))^+$ is expressed in the proposition below.

Proposition 2.4 [14, Proposition 3] *The contactomorphism ϕ from $(\mathbb{R}^3, \xi_{\mathrm{rot}})$ to $(\mathbb{R}^3, \xi_{\mathrm{std}})$ defined in Equation (1) sends the transverse link $T_{w(G)}$ to a link which is transversely isotopic to $(L(G))^+$.*

3 Link Floer homology and the transverse invariant

In this section, we describe the grid diagram formulation of link Floer homology discovered in [16; 17]. Let G be a grid diagram for a link L and suppose that G has

grid number k. From this point forward, we think of G as a *toroidal* grid diagram – that is, we identify the top and bottom sides of G and the right and left sides of G – so that the horizontal and vertical lines become k horizontal and k vertical circles. Let $\mathbb{O}$ and $\mathbb{X}$ denote the sets of markings $\{O_i\}_{i=1}^k$ and $\{X_i\}_{i=1}^k$, respectively.

We associate to G a chain complex $(CFL^-(m(L)), \partial^-)$ as follows. The generators of $CFL^-(L)$ are one-to-one correspondences between the horizontal and vertical circles of G. Equivalently, we may think of a generator as a set of k intersection points between the horizontal and vertical circles, such that no intersection point appears on more than one horizontal circle or on more than one vertical circle. We denote this set of generators by $\mathbf{S}(G)$. Then, $CFL^-(m(L))$ is defined to be the free $\mathbb{Z}_2[U_1, \ldots, U_k]$–module generated by the elements of $\mathbf{S}(G)$, where the U_i are formal variables corresponding to the markings O_i.

For $\mathbf{x}, \mathbf{y} \in \mathbf{S}(G)$, we let $\mathrm{Rect}_G(\mathbf{x}, \mathbf{y})$ denote the space of embedded rectangles in G with the following properties. $\mathrm{Rect}_G(\mathbf{x}, \mathbf{y})$ is empty unless $\mathbf{x}$ and $\mathbf{y}$ coincide at $k - 2$ points. An element $r \in \mathrm{Rect}_G(\mathbf{x}, \mathbf{y})$ is an embedded disk on the toroidal grid G whose edges are arcs on the horizontal and vertical circles and whose four corners are intersection points in $\mathbf{x} \cup \mathbf{y}$. Moreover, we stipulate that if we traverse each horizontal boundary component of r in the direction specified by the induced orientation on ∂r, then this horizontal arc is oriented from a point in $\mathbf{x}$ to a point in $\mathbf{y}$. If $\mathrm{Rect}_G(\mathbf{x}, \mathbf{y})$ is nonempty, then it consists of exactly two rectangles. See Figure 3 for an example. We let $\mathrm{Rect}_G^o(\mathbf{x}, \mathbf{y})$ denote the space of $r \in \mathrm{Rect}_G^o(\mathbf{x}, \mathbf{y})$ for which $r \cap \mathbb{X} = \mathrm{Int}(r) \cap \mathbf{x} = \varnothing$.
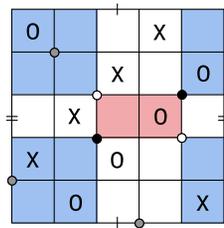

Figure 3: A grid diagram G for the right-handed trefoil. The generator $\mathbf{x}$ comprises the black and gray intersection points while $\mathbf{y}$ comprises the white and gray intersection points. $\mathrm{Rect}_G(\mathbf{x}, \mathbf{y})$ contains the shaded rectangles in red and blue, while $\mathrm{Rect}_G^o(\mathbf{x}, \mathbf{y})$ contains only the red rectangle.

The module $CFL^-(m(L))$ is endowed with an endomorphism

$$\partial^- : CFL^-(m(L)) \to CFL^-(m(L)),$$

defined on $\mathbf{S}(G)$ by

$$\partial^-(\mathbf{x}) = \sum_{\mathbf{y} \in \mathbf{S}(G)} \sum_{r \in \mathrm{Rect}^O_G(\mathbf{x}, \mathbf{y})} U_1^{O_1(r)} \cdots U_k^{O_n(r)} \cdot \mathbf{y}.$$

Here, $O_i(r)$ denotes the number of times the marking O_i appears in r. The map ∂^- is a differential, and, so, gives rise to a chain complex $(CFL^-(m(L)), \partial^-)$. The homology of this chain complex, $HFL^-(m(L)) = H_*(CFL^-(m(L)), \partial^-)$, is an invariant of the link L, and agrees with the *link Floer homology* of $m(L)$ defined in [24]. It bears mentioning that the complex $(CFL^-(m(L), \partial^-)$ comes equipped with *Maslov* and *Alexander* gradings, which are then inherited by $HFL^-(m(L))$; however, we will not discuss these gradings further as they play no role in this paper.

Suppose that the link L has l components. If O_i and O_j lie on the same component of L, then multiplication by U_i in $(CFL^-(m(L)), \partial^-)$ is chain homotopic to multiplication by U_j, and, so, these multiplications induce the same maps on $HFL^-(m(L))$ [17, Lemma 2.9]. So, if we label the markings in $\mathbb{O}$ so that $O_1, \ldots, O_l$ lie on different components, then we can think of $HFL^-(m(L))$ as a module over $\mathbb{Z}_2[U_1, \ldots, U_l]$.

Setting $U_1 = \cdots = U_l = 0$, one obtains a chain complex $(\widehat{CFL}(m(L)), \widehat{\partial})$ whose homology we denote by $\widehat{HFL}(m(L))$. The latter is a bigraded vector space over $\mathbb{Z}_2$, whose graded Euler characteristic is some normalization of the multivariable Alexander polynomial of $m(L)$ [24]. If one sets $U_1 = \cdots = U_k = 0$, one obtains a chain complex $(\widetilde{CFL}(m(L)), \widetilde{\partial})$ whose homology we denote by $\widetilde{HFL}(m(L))$. The group $\widetilde{HFL}(m(L))$ determines $\widehat{HFL}(m(L))$. Specifically, if we let n_i, for $i = 1, \ldots, l$, denote the number of markings in $\mathbb{O}$ on the i–th component of L, then

$$\widetilde{HFL}(m(L)) = \widehat{HFL}(m(L)) \otimes \bigotimes_{i=1}^{l} V_i^{\otimes(n_i - 1)},$$

where V_i is a fixed two dimensional vector space [17, Proposition 2.13], and the quotient map

$$j\colon \widehat{CFL}(m(L)) \to \widetilde{CFL}(m(L))$$

induces an injection j_* on homology.

The element $\mathbf{z}^+(G) \in \mathbf{S}(G)$, which consists of the intersection points at the upper right corners of the squares in G containing the markings in $\mathbb{X}$, is clearly a cycle in $(CFL^-(m(L)), \partial^-)$ (and, hence, also in the other chain complexes). If T is the transverse link in $(\mathbb{R}^3, \xi_{\mathrm{rot}})$ corresponding to the braid obtained from G as in Figure 2 (e), then T is topologically isotopic to L, and the image of $\mathbf{z}^+(G)$ in $HFL^-(m(T))$ is the transverse invariant $\theta^-(T)$ defined in [25]. The images of $\mathbf{z}^+(G)$ in $\widehat{HFL}(m(T))$ and $\widetilde{HFL}(m(T))$ are likewise denoted $\hat{\theta}(T)$ and $\tilde{\theta}(T)$, and are invariants of the transverse

link T as well. Moreover, the map j_* sends $\hat{\theta}(T)$ to $\tilde{\theta}(T)$; in particular, $\hat{\theta}(T) = 0$ if and only if $\tilde{\theta}(T) = 0$. The theorem below makes these statements about invariance precise.

Theorem 3.1 [25, Theorem 7.1] *Suppose that G and G' are two grid diagrams whose associated braids T and T' are transversely isotopic. Then, there is an isomorphism*

$$f_*^o \colon HFL^o(m(T)) \to HFL^o(m(T')),$$

induced by a chain map f^o, which sends $\theta^o(T)$ to $\theta^o(T')$.

Here, the superscript " ^{o} " is meant to indicate that this theorem holds for any of the three versions of link Floer homology described above. In particular, if T and T' are two transverse links for which $\hat{\theta}(T) \neq 0$ and $\hat{\theta}(T') = 0$, then T and T' are not transversely isotopic (the invariant $\theta^-(T)$ is always nonzero and non–U_i–torsion in $HFL^-(m(T))$ [25, Theorem 7.3]). These transverse invariants also behave nicely under negative braid stabilizations.

Theorem 3.2 [25, Theorem 7.2] *Suppose that G and G' are two grid diagrams with associated braids T and T', and suppose that T' is obtained from T by performing a negative braid stabilization along the i–th component of T. Then, there is an isomorphism*

$$f_*^- \colon HFL^-(m(T)) \to HFL^-(m(T')),$$

induced by a chain map f^-, which sends $\theta(T)$ to $U_i \cdot \theta(T')$.

Since multiplication by U_i is the same as multiplication by zero on $\widehat{HFL}$ and $\widetilde{HFL}$, we obtain the following corollary.

Corollary 3.3 *If T' is obtained from a transverse braid T by performing a negative braid stabilization along some component of T, then $\hat{\theta}(T') = \tilde{\theta}(T') = 0$.*

4 The map Φ and comultiplication

Fix some $w \in B_n$ and some $i \in \{1, \dots, n-1\}$. Figure 4 shows simultaneously a portion of a grid diagram G_β for $T_{w\sigma_i}$ and the corresponding portion of a grid diagram G_γ for T_w. The grid diagrams G_β and G_γ are the same except that G_β uses the horizontal curve β while G_γ uses the horizontal curve γ. Let k denote their common grid number.
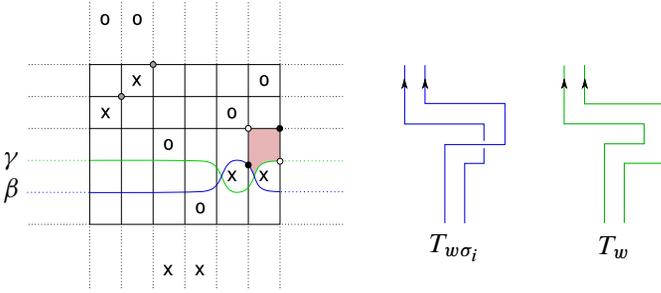
Figure 4: A portion of the grid diagrams G_β and G_γ. The cycle $\mathbf{z}^+(G_\beta)$ is shown as a collection of black and gray dots, while $\mathbf{z}^+(G_\gamma)$ is represented by the white and gray dots.

For $\mathbf{x} \in \mathbf{S}(G_\beta)$ and $\mathbf{y} \in \mathbf{S}(G_\gamma)$, let $\mathrm{Pent}_{\beta\gamma}(\mathbf{x}, \mathbf{y})$ denote the space of embedded pentagons with the following properties. $\mathrm{Pent}_{\beta\gamma}(\mathbf{x}, \mathbf{y})$ is empty unless $\mathbf{x}$ and $\mathbf{y}$ coincide at $k - 2$ points. An element $p \in \mathrm{Pent}_{\beta\gamma}(\mathbf{x}, \mathbf{y})$ is an embedded disk in the torus whose boundary consists of five arcs, each contained in horizontal or vertical circles. We stipulate that under the orientation induced on the boundary of p, the boundary may be traversed as follows. Start at the component of $\mathbf{x}$ on the curve β and proceed along an arc contained in β until we arrive at the right-most intersection point between β and γ; next, proceed along an arc contained in γ until we reach the component of $\mathbf{y}$ contained in γ; next, follow the arc of a vertical circle until we arrive at a component of $\mathbf{x}$; then, proceed along the arc of a horizontal circle until we arrive at a component of $\mathbf{y}$; finally, follow an arc contained in a vertical circle back to the initial component of $\mathbf{x}$. Let $\mathrm{Pent}^o_{\beta\gamma}(\mathbf{x}, \mathbf{y})$ denote the space of $p \in \mathrm{Pent}_{\beta\gamma}(\mathbf{x}, \mathbf{y})$ for which $p \cap \mathbb{X} = \mathrm{Int}(p) \cap \mathbf{x} = \varnothing$.

We construct a map

$$\phi^-: CFL^-(m(T_{w\sigma_i})) \to CFL^-(m(T_w))$$

of $\mathbb{Z}_2[U_1, \ldots, U_k]$–modules as follows. For $\mathbf{x} \in \mathbf{S}(G_\beta)$, let

$$\phi^-(\mathbf{x}) = \sum_{\mathbf{y} \in \mathbf{S}(G_\gamma)} \sum_{p \in \mathrm{Pent}^o_{\beta\gamma}(\mathbf{x},\mathbf{y})} U_1^{O_1(p)} \cdots U_k^{O_n(p)} \cdot \mathbf{y}.$$

We then define

$$\tilde{\phi}: \widetilde{CFL}(m(T_{w\sigma_i})) \to \widetilde{CFL}(m(T_w))$$

to be the map on $\widetilde{CFL}$ induced by ϕ^-. In other words, $\tilde{\phi}$ counts pentagons in $\mathrm{Pent}^o_{\beta\gamma}(\mathbf{x}, \mathbf{y})$ which also miss the $\mathbb{O}$ basepoints. (This construction is inspired by the proof of commutation invariance in [17, Section 3.1].)

Remark 4.1 Unlike $\tilde{\phi}$, the map ϕ^- is not necessarily a chain map.

The juxtaposition $p * r$ of any $p \in \text{Pent}^o_{\beta\gamma}(\mathbf{x}, \mathbf{y})$ with any rectangle $r \in \text{Rect}^o_{G_\gamma}(\mathbf{y}, \mathbf{w})$ such that $p \cap \mathbb{O} = r \cap \mathbb{O} = \varnothing$ has precisely one such decomposition and exactly one other decomposition as $r' * p'$, where $r' \in \text{Rect}^o_{G_\beta}(\mathbf{x}, \mathbf{y}')$ and $p' \in \text{Pent}^o_{\beta\gamma}(\mathbf{y}', \mathbf{w})$ and $r' \cap \mathbb{O} = p' \cap \mathbb{O} = \varnothing$. It follows that $\widetilde{\phi}$ is a chain map and, so, induces a map

$$\widetilde{\Phi}: \widetilde{HFL}(m(T_{w\sigma_i})) \to \widetilde{HFL}(m(T_w)).$$

Moreover, it is clear that $\text{Pent}^o_{\beta\gamma}(\mathbf{z}^+(G_\beta), \mathbf{z}^+(G_\gamma))$ consists only of the shaded pentagon shown in Figure 4, and that $\text{Pent}^o_{\beta\gamma}(\mathbf{z}^+(G_\beta), \mathbf{y})$ is empty for $\mathbf{y} \neq \mathbf{z}^+(G_\gamma)$. Therefore, $\widetilde{\Phi}$ sends $\widetilde{\theta}(T_{w\sigma_i})$ to $\widetilde{\theta}(T_w)$, proving Theorem 1.1.

The more general comultiplication fact stated in Theorem 1.2 follows from the above result together with the sequence of braid moves depicted in Figure 5: The braid in (a) represents the transverse link T_{hg}. The braid in (b) is obtained from that in (a) by a mixture of isotopy and positive stabilizations. The braid in (c) is obtained from that in (b) by isotopy followed by the introduction of negative crossings. The braid in (e) is isotopic to the braids in (c) and (d), and represents the connected sum of the transverse links T_g and T_h (for the latter statement, see Birman and Menasco [4]). Therefore, a composition of the maps $\widetilde{\Phi}$ described above (one for each negative crossing introduced in going from (b) to (c)) yields a map

$$\widetilde{\mu}: \widetilde{HFL}(m(T_{hg})) \to \widetilde{HFL}(m(T_g \# T_h))$$

which sends $\widetilde{\theta}(T_{hg})$ to $\widetilde{\theta}(T_g \# T_h)$.
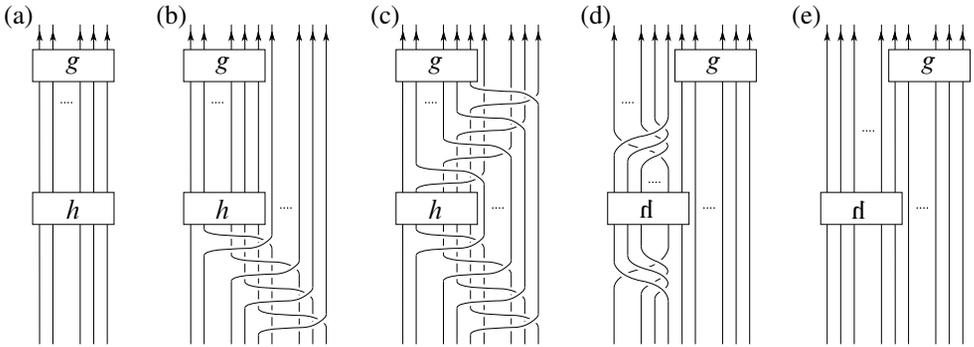

Figure 5: T_{hg} is transversely isotopic to the braid in (b), which, after introducing negative crossings (or, equivalently, up to braid isotopy, getting rid of positive crossings) is transversely isotopic to $T_g \# T_h$, which is represented by the braid in (e).

Suppose that $T_g \# T_h$ is any connected sum of T_g and T_h. In [28], Vértesi proves the following refinement of the Künneth formula described in [24, Theorem 1.4]. (Her

proof is actually for the analogous result in knot Floer homology, but it extends in an obvious manner to a proof of the theorem below.)

Theorem 4.2 *There is an isomorphism*

$$\widehat{HFL}(m(T_g \# T_h)) \cong \widehat{HFL}(m(T_g)) \otimes_{\mathbb{Z}_2} \widehat{HFL}(m(T_h))$$

under which $\hat{\theta}(T_g \# T_h)$ *is identified with* $\hat{\theta}(T_g) \otimes \hat{\theta}(T_h)$.

Vértesi's theorem, used in combination with the comultiplication map $\tilde{\mu}$, may be applied to prove Theorem 1.3.

Proof of Theorem 1.3 Recall from the previous section that $\hat{\theta}(T_w)$ is nonzero if and only if $\tilde{\theta}(T_w)$ is nonzero. If $\hat{\theta}(T_g)$ and $\hat{\theta}(T_h)$ are both nonzero, then, by Theorem 4.2, so is $\hat{\theta}(T_g \# T_h)$, and, hence, so is $\tilde{\theta}(T_g \# T_h)$. Since $\tilde{\mu}$ sends $\tilde{\theta}(T_{hg})$ to $\tilde{\theta}(T_g \# T_h)$ this implies that $\tilde{\theta}(T_{hg})$ is nonzero, and, hence, so is $\hat{\theta}(T_{hg})$. $\square$

Recall that a braid T_g is said to be *quasipositive* if $g \in B_n$ can be expressed as a product of conjugates of the form $w \sigma_i w^{-1}$, where w is any word in B_n.

Corollary 4.3 *If* T_g *is a quasipositive braid, then* $\hat{\theta}(T_g) \neq 0$.

Proof of Corollary 4.3 If g is a product of m conjugates as above, then after resolving the corresponding m positive crossings, one obtains a braid isotopic to I_n, the trivial $n-$braid. Therefore, a composition of m of the maps $\tilde{\Phi}$ sends $\tilde{\theta}(T_g)$ to $\tilde{\theta}(I_n)$. Moreover, one sees by glancing at the grid diagram for I_n in Figure 6 that $\tilde{\theta}(T_{I_n}) \neq 0$. Therefore, $\tilde{\theta}(T_g) \neq 0$ and the same is true of $\hat{\theta}(T_g)$. $\square$
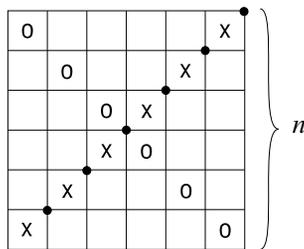

Figure 6: A grid diagram G_n for the trivial braid I_n. It is straightforward to check that the cycle $\mathbf{z}^+(G_n) \in \mathbf{S}(G_n)$, represented by the collection of black dots, is not a boundary in $\widetilde{CFL}(m(I_n))$.

Proof of Theorem 1.4 Suppose that T_w is a positive braid with one component. Then $\widehat{\theta}(T_w) \neq 0$, by the corollary above; also, T_w is a fibered knot [6]. Moreover, $\widehat{\theta}(T_w)$ lies in Alexander grading $(\mathrm{sl}(T_w) + 1)/2$, which, in this case, is simply the genus of T_w [25]. Therefore, $\widehat{\theta}(T_w)$ is the unique generator of $\widehat{HFL}(T_w, g(T_w))$. To show that $\widehat{\theta}(T_w) = \underline{\widehat{\theta}}(T_w)$, it suffices to prove that $\underline{\widehat{\theta}}(T_w)$ is nonzero as well. Fortunately, this has been shown by Vela-Vick in [27]. □

5 Finding new transversely nonsimple links

In this section, we outline and apply one strategy for using comultiplication (in particular, Theorem 1.3) to generate a plethora of new examples of transversely nonsimple link types. Consider the braid words

$$w_1 = a\sigma_1^m b\sigma_1^{-1} c \quad \text{and} \quad w_2 = a\sigma_1^{-1} b\sigma_1^m c$$

in B_n, where a, b and c are words in the generators $\sigma_2, \ldots, \sigma_{n-1}$. The transverse braids T_{w_1} and T_{w_2} are said to be related by a *negative flype* and, in particular, represent the same topological link type. If, in addition, m is odd, or if m is even and the two strands which cross according to σ_1^m belong to the same component of T_{w_1}, then $\mathcal{SL}(T_{w_1}) = \mathcal{SL}(T_{w_2})$.

Suppose that $\widehat{\theta}(T_{w_1}) = 0$ and $\widehat{\theta}(T_{w_2}) \neq 0$. The idea is to find a word h in the generators $\sigma_2, \ldots, \sigma_{n-1}$ with $\widehat{\theta}(T_h) \neq 0$. Theorem 1.3 would then imply that $\widehat{\theta}(T_{hw_2}) \neq 0$. If it is also true that $\widehat{\theta}(T_{hw_1}) = 0$, then T_{hw_1} and T_{hw_2} are not transversely isotopic although they are topologically isotopic. We would like to find examples which also satisfy $\mathcal{SL}(T_{hw_1}) = \mathcal{SL}(T_{hw_2})$ (if T_{hw_1} is a knot, this is automatic) so as to produce topological link types which are not transversely simple. One nice feature of this proposed method, which differs from that in [28], is that there is no reason to believe *a priori* that the link T_{hw_1} so obtained is composite.

In principle, Theorem 1.3 eliminates half of the work in this scenario – namely, showing that $\widehat{\theta}(T_{hw_2}) \neq 0$. In practice, one would like to find examples in which the other half – showing that $\widehat{\theta}(T_{hw_1})$ is zero – is very easy. To that end, one strategy is to pick an example in which T_{w_1} is transversely isotopic to a braid which can be negatively destabilized, and to show that the same is true of the braid T_{hw_1}, which would guarantee that $\widehat{\theta}(T_{hw_1}) = 0$ by Corollary 3.3. In particular, T_{w_1} must belong to a topological link type with a transverse representative (that is, T_{w_2}) which does not maximize self-linking number, but which cannot be negatively destabilized.

The most well-known such link type is that of the $(2, 3)$ cable of the $(2, 3)$ torus knot. In [12], Etnyre and Honda prove the following.

Proposition 5.1 *The $(2, 3)$ cable of the $(2, 3)$ torus knot has two Legendrian representatives, L_1 and L_2, both with $tb = 5$ and $r = 2$, for which L_1 is the positive (Legendrian) stabilization of a Legendrian knot while L_2 is not. Moreover, L_1 and L_2 are not Legendrian isotopic after any number of negative (Legendrian) stabilizations.*

That L_1 and L_2 are not Legendrian isotopic after any number of negative stabilizations implies that their transverse pushoffs, L_1^+ and L_2^+, are not transversely isotopic (yet, they both have $sl = 3$). Moreover, since L_1 is the positive stabilization of a Legendrian knot, its pushoff L_1^+ is transversely isotopic to the negative stabilization of some transverse braid.

Matsuda and Menasco have since given explicit forms for L_1 and L_2 [18]. Figures 7 (a) and 7 (a′) depict the rectangular diagrams corresponding to slightly modified versions of these forms (ours are derived from the front diagrams in [20, Figure 6]). The
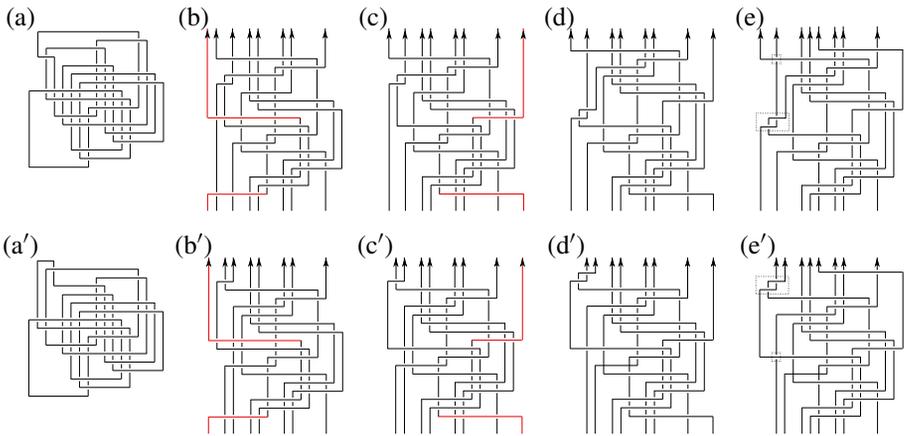

Figure 7: On the top, the rectangular diagrams for L_1 and its transverse pushoff L_1^+. On the bottom, those for L_2 and L_2^+. The circled regions in (e) and (e′) indicate that L_1^+ and L_2^+ are transversely isotopic to braids related by a negative flype.

rectangular braid diagrams for the transverse pushoffs L_1^+ and L_2^+ are shown in (b) and (b′), respectively. The braids in (c) and (c′) are obtained from those in (b) and (b′) by isotoping the red arcs as indicated, and the braids in (d) and (d′) are obtained from those in (c) and (c′) after additional simple isotopies and conjugations. The braids in (e) and (e′) are obtained from those in (d) and (d′) by conjugation, and they are related to one another by a negative flype. Indeed, Figure 7 shows that L_1^+ and L_2^+ are transversely isotopic to the transverse braids T_{w_1} and T_{w_2}, respectively, where

$$w_1 = a\sigma_1^2 b\sigma_1^{-1}c, \ w_2 = a\sigma_1^{-1}b\sigma_1^2 c,$$

$$a = \sigma_4\sigma_3\sigma_5\sigma_6\sigma_4\sigma_5\sigma_5\sigma_6\sigma_4\sigma_5\sigma_7\sigma_6\sigma_5^{-1}\sigma_4^{-1}\sigma_3^{-1}\sigma_2\sigma_3\sigma_3\sigma_4\sigma_5\sigma_4^{-1}\sigma_3^{-1}\sigma_2^{-1},$$

$$b = \sigma_5\sigma_6\sigma_7\sigma_6^{-1}\sigma_5^{-1}\sigma_4^{-1}\sigma_6^{-1}\sigma_5^{-1}\sigma_4^{-1}\sigma_3\sigma_4\sigma_5\sigma_2\sigma_3\sigma_4\sigma_4\sigma_5\sigma_6\sigma_5^{-1}\sigma_4^{-1}\sigma_3^{-1}\sigma_2^{-1},$$

$$c = \sigma_7^{-1}\sigma_6^{-1}\sigma_5^{-1}.$$

According to Proposition 5.1, T_{w_1} is transversely isotopic to a braid which can be negatively destabilized. Figure 8 shows a sequence of transverse braid moves which demonstrates that the same is true of T_{hw_1} for any word $h \in B_8$ in the generators $\sigma_3, \ldots, \sigma_6$. The braid in (b) is obtained from that in (a) by isotoping the red and blue
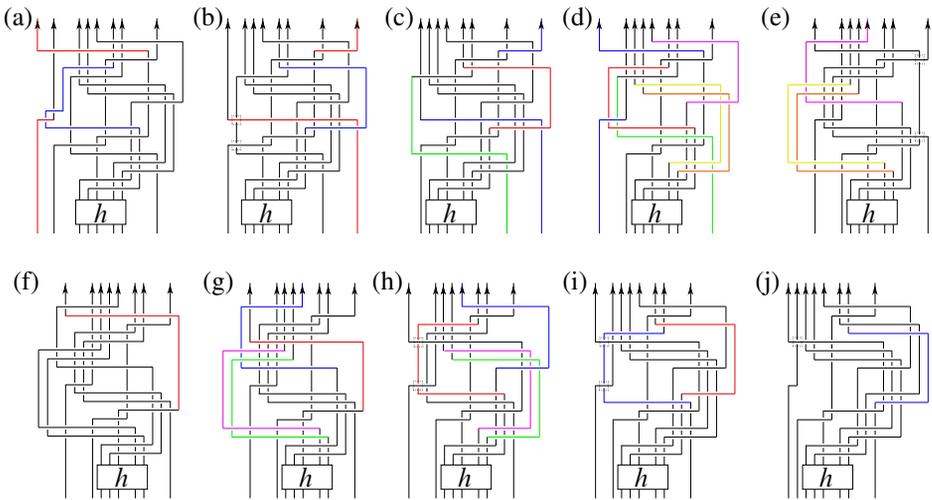

Figure 8: (a) shows a rectangular braid diagram for T_{hw_1}. After a sequence of braid isotopies and exchange moves, we obtain the braid in (j), which can be negatively destabilized.

arcs as shown. The braid in (c) is related to that in (b) by an exchange move at the circled crossings in (b). The braid in (d) is obtained from that in (c) by isotopy of the red, blue and green arcs. The braid in (e) is obtained from that in (d) after the indicated isotopy of the yellow, orange and purple arcs. An exchange move at the circled crossings in (e) produces the braid in (f). The braid in (g) is obtained from that in (f) by isotoping the red arc as shown. The braid in (h) is obtained from that in (g) after an isotopy of the blue, green and purple arcs as shown. An exchange move at the circled crossings in (h), followed by the indicated isotopy of the red arc produces the braid in (i). Finally, the braid in (j) is obtained from that in (i) by an exchange move at the circled crossings in (i), followed by the indicated isotopy of the blue arc.

Note that the braid in (j) may be negatively destabilized at the circled crossing. The essential point here is that the region of the braid in (a) corresponding to the word h is not affected by this combination of isotopies and exchange moves.

To sum up: since $\hat{\theta}(T_{w_2}) \neq 0$ (see Ng, Ozsváth and Thurston [20]), we have proven that for any $h \in B_8$ which is (1) a word in the generators $\sigma_3, \ldots, \sigma_6$ and for which (2) $\hat{\theta}(T_h) \neq 0$, it is the case that $\hat{\theta}(T_{hw_1}) = 0$ while $\hat{\theta}(T_{hw_2}) \neq 0$. It follows that the transverse braids T_{hw_1} and T_{hw_2} are not transversely isotopic though they are topologically isotopic. If, in addition, (3) h is such that the two strands of T_{hw_1} which cross according to the string σ_1^2 belong to the same component of T_{hw_1}, then $SL(T_{hw_1}) = SL(T_{hw_2})$; that is, the topological link type represented by T_{hw_1} is transversely nonsimple.

There are infinitely many choices of h which meet criteria (1)–(3) above. In order to give such an h, we first prove the following.

Lemma 5.2 For $1 \leq j \leq k$ and $0 \leq l \leq k - j$, consider the map $\psi_{j,k,l} : B_j \to B_k$ which sends σ_i to σ_{i+l}. If g is a word in B_j for which $\hat{\theta}(T_g) \neq 0$, and $h = \psi_{j,k,l}(g)$, then $\hat{\theta}(T_h) \neq 0$ as well.

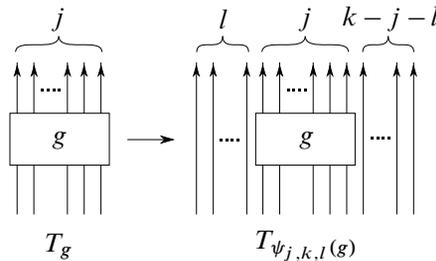See Figure 9 for a pictorial depiction of the map $\psi_{j,k,l}$.

Figure 9: On the left, the j–braid T_g. On the right, the k–braid $T_{\psi_{j,k,l}(g)}$.

Proof of Lemma 5.2 If $h = \psi_{j,k,l}(g)$, then the braid T_h is easily seen to be connected sum of T_g with the trivial braids $I_{k-j-l+1}$ and I_{l+1}. We know, from the proof of Corollary 4.3, that $\hat{\theta}(I_n) \neq 0$ for any $n \geq 1$. Lemma 5.2 therefore follows from Theorem 4.2. $\qquad\square$

It follows from Corollary 4.3 and from Lemma 5.2 that $h = \psi_{4,8,3}(g)$ satisfies criteria (1) and (2) above as long as T_g is a quasipositive 4–braid. Let $h = \psi_{4,8,3}(g)$ for

$$g = \sigma_3\sigma_2\sigma_3\sigma_1\sigma_2\sigma_3.$$

It is easy to check that h^n also satisfies criterion (3) (as well as criteria (1) and (2), of course) for all $n \geq 0$.

Corollary 5.3 *The topological link types represented by $T_{h^n w_1}$ are transversely nonsimple for all $n \geq 0$. When n is even, $T_{h^n w_1}$ is a knot; otherwise, $T_{h^n w_1}$ is a 3–component link.*

Below, we prove that most of the links in Corollary 5.3 are prime. Note that $T_{h^n w_1}$ is obtained from T_{w_1} by performing n positive half twists of strands 4–7 in the region of T_{w_1} where we would insert the word h^n. For $n = 2m$, this amounts to adding m positive full twists, which can also be accomplished by performing $-1/m$ surgery on an unknot U encircling strands 4–7 of T_{w_1} in the corresponding region. See Figure 10.
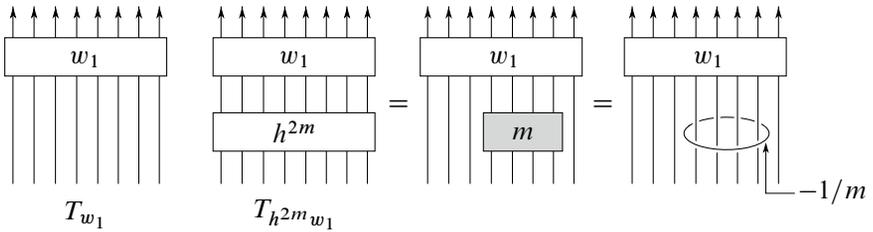

Figure 10: $T_{h^{2m} w_1}$ is obtained from T_{w_1} by performing m positive full twists of strands 4–7, or, equivalently, by performing $-1/m$ surgery on the unknot shown on the right.

A SnapPea computation [29] combined with the Inverse Function Theorem test described in Moser's thesis [19] shows that the complement of the link $T_{w_1} \cup U$ is hyperbolic. To be specific, SnapPea finds a triangulation of this link complement by ideal tetrahedra and computes an approximate solution to the gluing equations. Moser's test then confirms, using this approximate solution, that an exact solution exists.

Thurston's celebrated Dehn Surgery Theorem then implies that all but finitely many Dehn fillings of the boundary component corresponding to U are hyperbolic as well [26]. In turn, this implies that the link $T_{h^{2m} w_1}$ is hyperbolic, and, hence, prime for all but finitely many m. This argument can be repeated to show that the links $T_{h^{2m+1} w_1}$ are also prime for all but finitely many m. The lemma below sums this up.

Lemma 5.4 *The links $T_{h^n w_1}$ are prime for all but finitely many values of n.*

References

[1] **K Baker**, **J B Etnyre**, **J Van Horn-Morris**, *Fibered transverse knots and the Bennequin bound* arXiv:0803.0758

[2] **J A Baldwin**, *Comultiplicativity of the Ozsváth–Szabó contact invariant*, Math. Res. Lett. 15 (2008) 273–287   MR2385640

[3] **D Bennequin**, *Entrelacements et équations de Pfaff*, from: "Third Schnepfenried geometry conference, Vol. 1 (Schnepfenried, 1982)", Astérisque 107, Soc. Math. France, Paris (1983) 87–161   MR753131

[4] **J S Birman**, **W W Menasco**, *Studying links via closed braids. IV. Composite links and split links*, Invent. Math. 102 (1990) 115–139   MR1069243

[5] **J S Birman**, **W W Menasco**, *Stabilization in the braid groups. II. Transversal simplicity of knots*, Geom. Topol. 10 (2006) 1425–1452   MR2255503

[6] **J S Birman**, **R F Williams**, *Knotted periodic orbits in dynamical systems. I. Lorenz's equations*, Topology 22 (1983) 47–82   MR682059

[7] **Y Eliashberg**, *Legendrian and transversal knots in tight contact 3–manifolds*, from: "Topological methods in modern mathematics (Stony Brook, NY, 1991)", (L R Goldberg, A V Phillips, editors), Publish or Perish, Houston (1993) 171–193   MR1215964

[8] **J Epstein**, **D Fuchs**, **M Meyer**, *Chekanov–Eliashberg invariants and transverse approximations of Legendrian knots*, Pacific J. Math. 201 (2001) 89–106   MR1867893

[9] **J B Etnyre**, *Transversal torus knots*, Geom. Topol. 3 (1999) 253–268   MR1714912

[10] **J B Etnyre**, **K Honda**, *Knots and contact geometry. I. Torus knots and the figure eight knot*, J. Symplectic Geom. 1 (2001) 63–120   MR1959579

[11] **J B Etnyre**, **K Honda**, *On connected sums and Legendrian knots*, Adv. Math. 179 (2003) 59–74   MR2004728

[12] **J B Etnyre**, **K Honda**, *Cabling and transverse simplicity*, Ann. of Math. (2) 162 (2005) 1305–1333   MR2179731

[13] **K Kawamuro**, *Connect sum and transversely nonsimple knots*, Math. Proc. Cambridge Philos. Soc. 146 (2009) 661–669   MR2496350

[14] **T Khandhawit**, **L Ng**, *A family of transversely nonsimple knots*, Algebr. Geom. Topol. 10 (2010) 293–314

[15] **P Lisca**, **P Ozsváth**, **A Stipsicz**, **Z Szabó**, *Heegaard Floer invariants of Legendrian knots in contact three-manifolds*   arXiv:0802.0628

[16] **C Manolescu**, **P Ozsváth**, **S Sarkar**, *A combinatorial description of knot Floer homology*, Ann. of Math. (2) 169 (2009) 633–660   MR2480614

[17] **C Manolescu**, **P Ozsváth**, **Z Szabó**, **D Thurston**, *On combinatorial link Floer homology*, Geom. Topol. 11 (2007) 2339–2412   MR2372850

[18] **W W Menasco**, **H Matsuda**, *An addendum on iterated torus knots (appendix)*   arXiv:math.GT/0610566

[19] **H H Moser**, *Proving a manifold to be hyperbolic once it has been approximated to be so*, ProQuest LLC, Ann Arbor, MI (2005) MR2621880 PhD Thesis–Columbia University

[20] **L Ng**, **P Ozsváth**, **D Thurston**, *Transverse knots distinguished by knot Floer homology*, J. Symplectic Geom. 6 (2008) 461–490 MR2471100

[21] **L Ng**, **D Thurston**, *Grid diagrams, braids, and contact geometry*, from: "Proceedings of Gökova Geometry-Topology Conference 2008", (S Akbulut, T Önder, R J Stern, editors) (2009) 120–136 MR2500576

[22] **S Y Orevkov**, **V V Shevchishin**, *Markov theorem for transversal links*, J. Knot Theory Ramifications 12 (2003) 905–913 MR2017961

[23] **P Ozsváth**, **A Stipsicz**, *Contact surgeries and the transverse invariant in knot Floer homology* arXiv:0803.1252

[24] **P Ozsváth**, **Z Szabó**, *Holomorphic disks, link invariants and the multi-variable Alexander polynomial*, Algebr. Geom. Topol. 8 (2008) 615–692 MR2443092

[25] **P Ozsváth**, **Z Szabó**, **D Thurston**, *Legendrian knots, transverse knots and combinatorial Floer homology*, Geom. Topol. 12 (2008) 941–980 MR2403802

[26] **W P Thurston**, *The geometry and topology of three-manifolds*, Princeton Univ. Math. Dept. Lecture Notes (1979) Available at http://msri.org/publications/books/gt3m/

[27] **D S Vela-Vick**, *On the transverse invariant for bindings of open books* arXiv:0806.1729

[28] **V Vértesi**, *Transversely nonsimple knots*, Algebr. Geom. Topol. 8 (2008) 1481–1498 MR2443251

[29] **J Weeks**, *SnapPea* Available at http://www.geometrygames.org/SnapPea

[30] **N Wrinkle**, *The Markov theorem for transverse knots* arXiv:math.GT/0202055

Department of Mathematics, Princeton University
Princeton, NJ 08544-1000

baldwinj@math.princeton.edu

http://www.math.princeton.edu/~baldwinj